

## Microscopic Origin of Liquid Crystal Alignment on Rubbed Polymer Surfaces

J. Stöhr,<sup>\*,†</sup> M. G. Samant,<sup>†</sup> A. Cossy-Favre,<sup>‡</sup> J. Díaz,<sup>‡</sup> Y. Momoi,<sup>§</sup> S. Odahara,<sup>§</sup> and T. Nagata<sup>||</sup>

Almaden Research Center, IBM Research Division, 650 Harry Road, San Jose, California 95120, Advanced Light Source, Lawrence Berkeley National Laboratory, Berkeley, California 94720, Display Technology, IBM Japan, 1623-14 Shimotsuruma, Yamato-shi, Kanagawa-ken 242, Japan, and Materials Laboratory, IBM Japan, 1 Kirihara-cho, Fujisawa-shi, Kanagawa-ken 252, Japan

Received August 1, 1997; Revised Manuscript Received November 6, 1997

**ABSTRACT:** Surface-sensitive and polarization-dependent near-edge X-ray absorption fine structure (NEXAFS) measurements clearly reveal a preferred in-plane and out-of-plane orientation of phenyl and C=O groups at the surface of rubbed polyimide films. The unidirectional molecular alignment at the surface is argued to provide the template for liquid crystal (LC) alignment of the films. Both the LC orientation along the rubbing direction as well as the direction of the out-of-plane LC pretilt are explained in a simple model. In this model the LC direction follows the preferential orientation of the phenyl rings at the surface. The preferred phenyl orientation is explained in terms of preferential chain segment alignment through a pulling action of the rubbing cloth fibers. The proposed LC alignment model is based on the existence of a statistically significant unidirectional bond asymmetry at the polymer surface, and it does not require the existence of crystalline order.

### I. Introduction

The origin of the alignment of liquid crystal (LC) molecules on rubbed polymer surfaces has remained a puzzle since its discovery in 1911.<sup>1</sup> The alignment mechanism is not only an interesting scientific but an important technological problem, since today's flat panel displays are largely based on LCs that modulate light transmission from the back to the front of the display through changes in alignment.<sup>2,3</sup> In general, the LC alignment has to originate from symmetry breaking at the surface of the polymer substrate. Asymmetries in either the macroscopic topographical or microscopic molecular structure of the polymer surface have been proposed for its origin.<sup>4</sup> While a variety of methods can be used to determine the precise alignment direction of the LC molecules, even for monolayer films,<sup>5</sup> it is more difficult to obtain detailed information regarding the molecular structure of the polymer surface.

Early proposals of the molecular orientation at the polymer surface were based on bulk-sensitive optical measurements.<sup>6–11</sup> Recently, surface-sensitive studies have been carried out using the near-edge X-ray absorption fine structure (NEXAFS)<sup>12–15</sup> and grazing incidence X-ray scattering (GIXS)<sup>16</sup> techniques. Both NEXAFS<sup>15</sup> and GIXS<sup>16</sup> studies on BPDA–PDA polyimide demonstrated the preferential near-surface alignment of polyimide chain segments along the rubbing direction, linking it to the preferred in-plane alignment direction of the LCs. Because BPDA–PDA polyimide is partially ordered (semicrystalline), the question has remained unanswered whether the LC alignment mechanism is different in disordered polymers where no structural correlation exists between the chains. Such polymers are typically used in technological applications.

Another important aspect of LC alignment, namely the origin of the so-called pretilt angle  $\epsilon$  illustrated in Figure 1, also remains ill understood. The pretilt angle is of great technological importance in that it determines the gray scale contrast in LC displays. The origin of both the tilt *direction*, which for polyimide substrates is always found to point up into the rubbing direction, as shown in Figure 1, and the *size* of the tilt angle  $\epsilon$  are of interest. Previous NEXAFS studies on BPDA–Cn and PMDA–Cn polyimides<sup>12,14</sup> linked the LC pretilt angle to a tilt angle of the aromatic building blocks at the polyimide surface. In another study the size of the pretilt angle has been explained in terms of the van der Waals interaction between the first LC monolayer and the polymer surface, independent of any asymmetry at the polymer surface.<sup>17</sup> Because this theory models the surface as a semiinfinite dielectric medium without any anisotropy on a molecular level, it cannot account for the LC tilt direction.

Here we report surface-sensitive and polarization-dependent NEXAFS measurements that clearly reveal a preferential asymmetric in-plane and out-of-plane alignment of C=O and phenyl groups at the polyimide surface. This preferred molecular orientation exists even though the polymer is disordered. In particular, the observed asymmetric out-of-plane tilt is argued to be the microscopic origin of the LC pretilt direction. In our model, the LC axis is parallel to and guided by the preferentially oriented phenyl planes at the polymer surface, without the requirement of crystalline order. We also present a simple model that links the asymmetric molecular orientation at the polyimide surface to the rubbing process.

### II. Experimental Details

NEXAFS measurements were performed at the Stanford Synchrotron Radiation Laboratory on the wiggler beam line 10-1 using nearly linearly polarized soft X-rays with an energy resolution of  $\sim 100$  meV at the carbon K-edge. NEXAFS spectra were recorded in the same experimental geometry as

<sup>†</sup> IBM Research Division.

<sup>‡</sup> Lawrence Berkeley National Laboratory.

<sup>§</sup> Display Technology, IBM Japan.

<sup>||</sup> Materials Laboratory, IBM Japan.

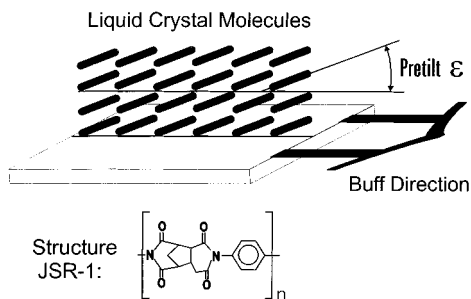


**Figure 1.** Illustration of the liquid crystal in-plane orientation along the rubbing direction and the out-of-plane pretilt angle  $\epsilon$ . The monomer unit of the investigated polyimide is also shown.

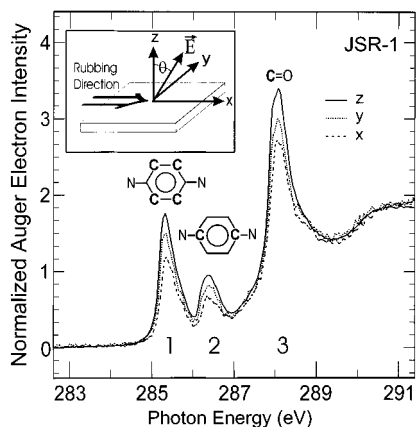


**Figure 2.** NEXAFS spectra recorded for sample JSR-1 with  $\vec{E} \parallel x$  (dashed line),  $y$  (dotted line) and  $20^\circ$  from the  $z$  axis (solid line). The experimental geometry is shown in the inset. The buffing direction is taken along the  $x$  axis. By rotation of the sample around the  $z$  axis, the  $\vec{E}$  vector of the incident X-rays could be oriented in either the  $x$ - $z$  plane or  $y$ - $z$  plane. The polar angle  $\theta$  was changed by rotating the sample about an axis in the surface plane. The assignment of the observed peaks 1–3 to  $\pi^*$  orbitals of chemically different C atoms is also indicated.

in our earlier measurements.<sup>15</sup> As shown in the inset of Figure 2, the major component of the electric field vector  $\vec{E}$  of the X-rays was oriented either parallel ( $\vec{E} \parallel x$ ) or perpendicular ( $\vec{E} \parallel y$ ) to the rubbing direction, at an angle  $\theta$  from the sample normal  $z$ . We used KLL Auger electron yield detection, which probes only the first nanometer from the free surface.<sup>15,18</sup> Simultaneously, we recorded total electron yield spectra,<sup>15</sup> which probe about 10 nm below the surface, but they are not reported here. The spectra were normalized to the incident photon flux and to the number of C atoms in the sample, as discussed elsewhere.<sup>15,19</sup>

We investigated the Japan Synthetic Rubber (JSR) polyimide JALS-146-R19, whose structure is shown in Figure 1. We shall refer to this polyimide as JSR-1 below. The polymer was dissolved in an organic solvent and spin coated onto  $10 \times 10$  cm<sup>2</sup> indium–tin–oxide-coated glass plates to a thickness of less than 100 nm. After heating to  $85^\circ\text{C}$  to remove the solvent, the samples were baked at  $180^\circ\text{C}$  for 60 min. Some samples were rubbed using a rayon-cloth rubbing machine at 200 rpm rotation speed, 25 mm/s plate speed, and a pile impression of 0.6 mm. For the NEXAFS measurements we used  $1 \times 1$  cm<sup>2</sup> pieces, cut from the unrubbed and rubbed sample plates.

### III. Experimental Results

NEXAFS spectra for sample JSR-1 are shown in Figure 2 for three orientations of the  $\vec{E}$  vector, along  $x$ ,  $y$ , and  $20^\circ$  from the  $z$  axis. The observed peaks 1–3 can be assigned to transitions to  $\pi^*$  orbitals on specific C atoms, as indicated in the figure.<sup>15,19</sup> From the angular

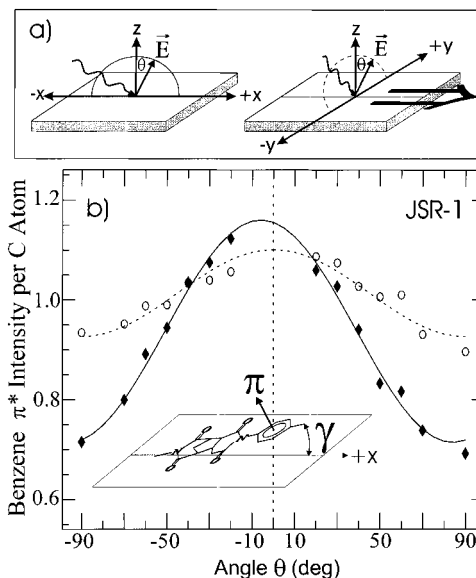


**Figure 3.** (a) Measurement geometry. The polar angle  $\theta$  is taken positive for  $\vec{E}$  in the  $(+x, z)$  and  $(+y, z)$  and negative for  $\vec{E}$  in the  $(-x, z)$  and  $(-y, z)$  quadrants, respectively. (b) The peak 1 NEXAFS intensity measured in the  $(-x, z, +x)$  plane is shown as diamonds. The solid line is a fit using eq 1. The open circles correspond to the measured peak 1 intensity for  $\vec{E}$  in the  $(-y, z, +y)$  plane, perpendicular to the rubbing direction, and the dashed line is a fit using eq 2. The inset illustrates the out-of-plane tilt angle  $\gamma$  of the phenyl rings at the polyimide surface revealed by the asymmetric  $\pi^*$  intensity distribution in the  $(-x, z, +x)$  plane.

dependence of the peak intensities, one can derive the preferential orientation of the corresponding  $\pi$  orbitals. For example, peak 1 originates from  $1s \rightarrow \pi^*$  electronic transitions on the central four C atoms in the phenyl rings. It has maximum intensity when the  $\vec{E}$  vector is parallel to the phenyl  $\pi$  system, i.e., perpendicular to the phenyl ring.<sup>15,19</sup> The spectra in Figure 2 show a significant asymmetry in the number of phenyl and C=O  $\pi$  orbitals oriented along the  $x$ ,  $y$ , and  $z$  directions at the rubbed polymer surface. The  $\pi$  orbitals are preferentially oriented along the surface normal, and there are more  $\pi$  orbitals oriented along  $y$  than  $x$ .

A more detailed look at the measured intensity distribution in the  $x$ - $z$  plane containing the rubbing direction is given in Figure 3. For the rubbed sample, the measured intensity of peak 1, shown as diamonds, is asymmetric with respect to the surface normal. The solid curve through the data points is a fit by the general NEXAFS intensity distribution function for a system with lower than 2-fold symmetry<sup>19</sup>

$$I^l(\theta) = A^l + B^l \sin^2 \theta + C^l \sin 2\theta \quad (1)$$

where the constants  $A^l = 1.16$ ,  $B^l = -0.437$ , and  $C^l = -0.0458$  depend on the angular distribution of the  $\pi$  orbitals and the X-ray polarization. The phenyl  $\pi$  intensity is peaked close to  $\theta = 0$ , indicating a preferential orientation of the  $\pi$  system along the surface normal but it is asymmetric in the  $(-x, z, +x)$  plane relative to the surface normal ( $\theta = 0$ ). This asymmetry arises from an asymmetric distribution of the phenyl  $\pi$  orbitals about the surface normal. The larger  $\pi$  resonance intensity for negative values of  $\theta$ , defined as a tilt of  $\vec{E}$  toward the  $-x$  axis, shows that, on average, the  $\pi$  orbitals are preferentially tilted from the  $z$  axis toward the  $-x$  axis. This is equivalent to a preferential

upward tilt of the phenyl planes from the  $+x$  axis by an angle  $\gamma$ , as illustrated in the inset of Figure 3b. This asymmetry is absent for the  $(-y, z, +y)$  plane, which is perpendicular to the buffing direction. The respective experimental data are shown as open circles in Figure 3b, and the dashed line is a fit using the equation

$$I^\perp(\theta) = A^\perp + B^\perp \sin^2 \theta \quad (2)$$

with  $A^\perp = 1.10$  and  $B^\perp = -0.175$ . We obtain nearly identical results for the asymmetries of the phenyl and C=O  $\pi$  intensities in all cases.

#### IV. Discussion

Figure 1 shows that for rubbed polyimides the LCs are aligned unidirectionally (i.e., their long axis is along the buffing direction  $x$ ) and they are tipped up from the buffing direction by the pretilt angle  $\epsilon$ . For polyimides, the same LC directionality exists, independent of the type of polyimide and LC material. It is therefore expected that the LC alignment *direction*, i.e., the in-plane as well as out-of-plane pretilt direction, is solely determined by the structural asymmetry at the polymer surface induced by rubbing. In contrast, the size of the pretilt angle depends on the type of polyimide and LC material.<sup>4</sup> Therefore, we can expect to find a direct relationship between the bond asymmetry at the polyimide surface and the LC alignment direction, while only a qualitative correlation is expected between the bond asymmetry and the *size of the pretilt angle*. Below we shall develop a quantitative description of the bond asymmetry at the polymer surface as determined by NEXAFS.

**A. Determination of Molecular Orientation at Surface.** We can quantitatively determine the average out-of-plane tilt angle  $\gamma$  of the phenyl planes, illustrated in Figure 3b, by realizing that eq 1 can be written in the form<sup>20</sup>

$$I^\parallel(\theta) = a^\parallel + b^\parallel \cos 2(\theta - \gamma) \quad (3)$$

where  $A^\parallel = a^\parallel + b^\parallel \cos 2\gamma$ ,  $B^\parallel = -2b^\parallel \cos 2\gamma$ , and  $C^\parallel = b^\parallel \sin 2\gamma$ . We see that our sample coordinate system  $x, y, z$  can simply be rotated into a new coordinate system  $x', y', z'$  by an angle  $\gamma$  about the  $y = y'$  axis. In this new coordinate system, the distribution function of the  $\pi$  orbitals has at least 2-fold symmetry about the new axes  $x', y'$ , and  $z'$ , while in the sample frame only a 1-fold rotational symmetry existed about the  $z$  axis. The rotation angle is given by

$$\tan 2\gamma = -2C^\parallel/B^\parallel \quad (4)$$

The tilt angle  $\gamma$  is determined by symmetry alone, and it is independent of the actual molecular distribution function. It is negative for clockwise rotation and positive for anticlockwise rotation about the  $y = y'$  axis. From the fit parameters we obtain the value  $\gamma = -5.9 \pm 0.5^\circ$  for JSR-1 polyimide.

Since the detailed molecular orientation function cannot be determined by NEXAFS,<sup>15</sup> we use concepts developed in conjunction with optical measurements<sup>21</sup> and characterize the orientational anisotropy by three orientation factors  $f_x, f_y$ , and  $f_z$ . Because of the 2-fold molecular symmetry in the  $(x', y', z')$  frame, the orientation factors are simply the projections of the molecular orientation function along the three axes. For a normalized distribution we have  $f_x + f_y + f_z = 1$  so that

Change of phenyl orientation by rubbing

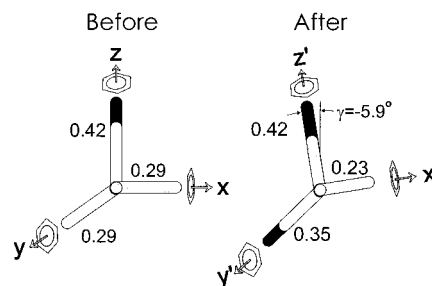


**Figure 4.** Relative number of phenyl rings, before and after rubbing, at the surface of sample JSR-1 with  $\pi$  orbitals directed along  $x', y'$ , and  $z'$ , derived from the NEXAFS data. For the rubbed sample the molecular tilt angle  $\gamma$  at the polymer surface is also given. The isotropic parts of the distributions are indicated in different shading.

the orientation factors represent the fractions of molecules with their  $\pi$  systems aligned along the  $x', y'$ , and  $z'$  axes, respectively, independent of the actual molecular distribution function.

For elliptically polarized X-rays, characterized by a polarization factor  $P$ <sup>19</sup> and a relative rotation of the  $(x', y', z')$  frame by an angle  $\gamma$  about the  $y = y'$  axis, we obtain the following equations for our experimental geometry,

$$f_x = \frac{A^\perp + B^\parallel \left(1 + \frac{\sin^2 \gamma}{P \cos 2\gamma}\right)}{I_{tot}} \quad (5)$$

$$f_y = \frac{A^\parallel + B^\perp}{I_{tot}} \quad (6)$$

$$f_z = \frac{A^\perp + B^\parallel \left(1 - \frac{\cos^2 \gamma}{P \cos 2\gamma}\right)}{I_{tot}} \quad (7)$$

The normalization condition  $f_x + f_y + f_z = 1$  yields the following expression for the total integrated intensity  $I_{tot}$

$$I_{tot} = \frac{3}{2}(A^\parallel + A^\perp) + \frac{3P-1}{2P}(B^\parallel + B^\perp) \quad (8)$$

The polarization factor can also be directly obtained as

$$P = \frac{B^\perp - B^\parallel}{A^\parallel - A^\perp + B^\perp - B^\parallel} \quad (9)$$

From the fit parameters we determine the polarization factor  $P = 0.82 \pm 0.05$ , which is close to the expected value  $P = 0.80$ .

The orientation factors determined from our measurements, assuming the theoretical value  $P = 0.80$ , are graphically shown in Figure 4. Error bars are about 2% of the listed values. We have plotted the relative number of phenyl rings with  $\pi$  orbitals directed along  $x', y'$ , and  $z'$ , before and after the rubbing process. Note that for the unrubbed sample the sample frame  $(x, y, z)$  coincides with the frame  $(x', y', z')$ . Similar distributions are obtained from the angular dependence of the measured peak 2 intensities associated with the  $\pi$  orbitals on the outer two phenyl C atoms (bonded to  $N$

neighbors) and for the intensities of peak 3 associated with the C=O  $\pi$ -system.

Figure 4 reveals that a preferential molecular orientation exists even before the rubbing process as a consequence of the symmetry breaking at the surface. The phenyl rings are preferentially oriented with their plane parallel to the surface. However, no in-plane asymmetry is observed for the unrubbed samples. The rubbing process leads to an in-plane redistribution of the phenyl  $\pi$  system from  $x'$  to  $y'$  without affecting the relative number of  $\pi$  orbitals along  $z'$ . Since on average, the phenyl and C=O  $\pi$  systems are oriented perpendicular to the polymer chain segment directions, Figure 4 indicates a preferred chain orientation along the buffing direction  $x$ .

From the orientation factors we may also determine the tensor order parameter  $Q^{\alpha\beta}$  (with  $\alpha, \beta = x', y',$  or  $z'$ ) for the rubbed polymer surface.<sup>20</sup> It is diagonal in the  $x', y',$  and  $z'$  frame and is defined as<sup>21</sup>

$$Q^{\alpha\beta} = \begin{pmatrix} -\frac{1}{2}(S + \eta) & 0 & 0 \\ 0 & -\frac{1}{2}(S - \eta) & 0 \\ 0 & 0 & S \end{pmatrix} = \begin{pmatrix} \frac{1}{2}(3f_x - 1) & 0 & 0 \\ 0 & \frac{1}{2}(3f_y - 1) & 0 \\ 0 & 0 & \frac{1}{2}(3f_z - 1) \end{pmatrix} \quad (10)$$

Here  $S$  is the uniaxial order parameter and  $\eta$  is the biaxiality.<sup>21</sup> The rubbed polymer surface can therefore be described by a biaxial distribution with unequal distributions along the  $x', y',$  and  $z'$  axes, as illustrated in Figure 4. We obtain  $S = 0.14 \pm 0.01$  and  $\eta = 0.17 \pm 0.01$ . In comparison, a nematic LC is described by a uniaxial distribution  $\eta = 0$ , with an order parameter in the  $0.4 < S < 0.7$  range.

**B. Liquid Crystal and Polymer Alignment.** Comparison of the known LC alignment direction with the preferential bond orientation at the surface of the polymer film revealed by the NEXAFS measurements suggests that the LC direction is determined by the preferential in- and out-of-plane bond orientation at the polymer surface. In our measurement, the preferential bond orientation is most clearly seen as an anisotropy of the phenyl or C=O  $\pi$  orbitals, as pictured in Figure 4, but the  $\sigma$  orbitals are, of course, anisotropic as well. The LC consists of rodlike units that typically contain in-line phenyl rings and a C $\equiv$ N group, and it has cylindrical symmetry about the average rod direction. Therefore, from a chemical point of view, one may describe the LC as an ensemble of long molecules with the  $\pi$  system lying in a plane perpendicular to the average rod direction.

Our data then suggest that the alignment originates from a  $\pi$ -like interaction between the LC and the anisotropic polymer surface. We do not imply the existence of a chemical  $\pi$  bond but merely mean that the attractive interaction between the polymer surface and the LC is in the direction of the respective  $\pi$  orbitals of the two interacting systems. The interaction orients the LCs with their  $\pi$  orbitals parallel to the preferred direction of the  $\pi$  orbitals of the phenyl or C=O groups at the polymer surface. We cannot tell whether the

phenyl or C=O groups are more important for the LC alignment since both show the same preferential orientation.

One can most easily visualize the directionality of the interaction by saying that the LC rods align parallel to the preferred orientation of the phenyl planes at the polyimide surface. In this picture, the preferred LC alignment along the buffing direction  $x$  is explained by the preferred phenyl plane orientation parallel to the  $x$ -axis, as shown in Figure 4. The out-of-plane tilt of the phenyl planes  $\gamma$ , depicted in the inset of Figure 3b, is the microscopic origin of the LC pretilt angle. It causes the LCs to tilt up from and point into the rubbing direction. The tilt angle at the polyimide surface  $|\gamma| = 5.9^\circ$  is larger than the LC pretilt angles  $\epsilon = 1.5^\circ$  measured with Merck ZLI-2293<sup>22</sup> and  $\epsilon = 2.2^\circ$  obtained by us with 5CB. As discussed above, in general, we cannot expect the existence of a quantitative relationship between the size of the bulk LC pretilt angle  $\epsilon$  and the phenyl ring tilt angle  $\gamma$  at the polyimide surface. We argue, however, that the LC pretilt direction is set by the surface asymmetry.

Our model is also supported by NEXAFS results for buffed polystyrene surfaces.<sup>23</sup> Here the phenyl ring planes are found to lie preferentially in the  $y$ - $z$  plane, perpendicular to the buffing direction, and this leads to the observed LC orientation perpendicular to the buffing direction.<sup>7,24</sup> Also, because the rubbing process does not cause an asymmetric molecular distribution about the  $z$  axis in the  $(-y, z, +y)$  plane, no directional pretilt is expected from our model, again in agreement with empirical observations.<sup>7</sup>

We note that, in general, the preferential bond orientation at the polymer surface is unrelated to crystalline order, i.e., the presence of structural correlation between the chains. Hence the LC alignment mechanism proposed here contrasts earlier beliefs that polymer crystallinity is necessary for LC alignment to occur.<sup>6</sup> Our model simply assumes the presence of a statistically significant preferential molecular orientation at the polymer surface. The anchoring energy of the LC to the surface is then minimized by a parallel alignment of the LC rods and the phenyl rings at the polymer surface.

**C. Molecular Reorientation by Rubbing.** Finally, we address the origin of the preferred molecular orientation at the polyimide surface caused by the rubbing process. Similar to the GIXS<sup>16</sup> and NEXAFS<sup>15</sup> results for BPDA-PDA polyimide, our results indicate a preferential chain segment orientation along the rubbing direction. This suggests that the rubbing process orients polymer chain segments at the surface in a similar manner as stretching does for a bulk polymer. A simple model for the orientation process suggested by our data is illustrated in Figure 5. The tips of the rubbing cloth fibers may be envisioned to pull on the surface segments of the polymer chains in the rubbing direction  $x$  (Figure 5a). One may also visualize the rubbing effect by a shearing of the surface, as proposed by Geary et al.<sup>6</sup> Both processes lead to a similar redistribution of the number of chain segments at the surface, increasing the number of segments along  $x$  relative to those along  $y$ , as illustrated in Figure 5b. Because for polyimides the chain segment axis is perpendicular to the phenyl  $\pi$  system, indicated by arrows in Figure 5b, this leads to more phenyl rings with their  $\pi$  orbitals along  $y$  than along  $x$ , as observed

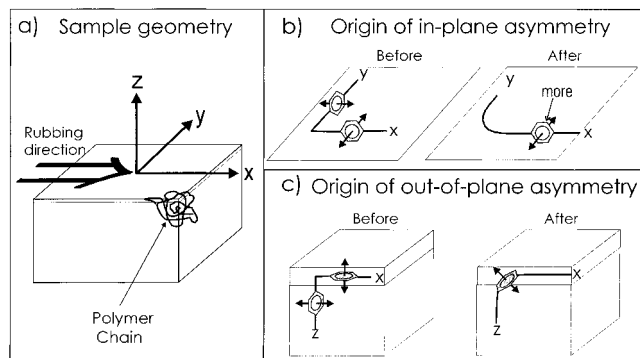


**Figure 5.** (a) Sample geometry during the rubbing process. (b) Illustration of chain segment motion and associated phenyl ring reorientation from before to after the rubbing process in the  $x$ - $y$  surface plane. (c) Chain segment motion and associated phenyl ring reorientation from before to after the rubbing process in the  $x$ - $z$  plane. This process leads to a preferential tilt of vertical phenyl planes toward the  $+x$  axis, as shown.

(see Figure 4). Note that the redistribution in chain segments from  $y$  to  $x$  does not change the number of phenyl rings with their  $\pi$  orbitals along  $z$ . This is supported by our results shown in Figure 4.

The origin of the out-of-plane asymmetry in the  $x$ - $z$  plane is illustrated in Figure 5c. Here we show chain segments initially oriented along  $x$  and  $z$  and only consider phenyl rings with their  $\pi$  systems in the  $x$ - $z$  plane, since only those can lead to the observed asymmetry. When the rubbing fibers pull on a chain segment oriented along  $x$ , a distortion in orientation will occur for the linked chain segments that are initially oriented along  $z$ . Thus, at the surface of the rubbed polyimide, a preferential tilting of the originally vertical chain segments and phenyl planes toward  $+x$  will result, as indicated in Figure 5c. From the model shown in Figure 5c one would therefore expect that the rubbing process leads to a preferential orientation of the phenyl  $\pi$  orbitals in the  $(-x, z)$  quadrant relative to that in the  $(+x, z)$  quadrant, as observed. Hence we predict that for all polyimide surfaces, the LCs will always align along the rubbing direction, and they will always tip up from the rubbing direction  $x$ , not from the opposite direction  $-x$ .

## V. Conclusions

We have presented NEXAFS measurements that clearly reveal the preferred orientation of phenyl and C=O groups at the surface of a rubbed polyimide film. This orientation is argued to be the microscopic origin for LC alignment on the surface. Both the preferred LC alignment direction parallel to the rubbing direction as well as the direction of the out-of-plane LC pretilt is explained by a simple model based on the preferential orientation of phenyl rings. The preferential molecular orientation at the polymer surface is explained in terms of a preferential chain segment alignment parallel to

the rubbing direction, caused by a pulling action of the rubbing fibers. Our model for LC alignment does not require the presence of crystalline order at the polymer surface but is solely based on the existence of a statistically significant bond asymmetry at the surface.

**Acknowledgment.** We would like to thank Yasuo Matsuki of Japan Synthetic Rubber for many useful discussions. J.D. thanks the Ministerio de Educacion y Ciencia of Spain for financial support. The work was carried out at SSRL, which is operated by the U.S. Department of Energy.

## References and Notes

- (1) Mauguin, C. *Bull. Soc. Fr. Miner.* **1911**, *34*, 71.
- (2) Depp, S. W.; Howard, W. E. *Sci. Am.* **1993**, *268*, 90.
- (3) For reviews of various aspects of thin-film-transistor liquid crystal display technology see: *IBM J. Res. Dev.* **1992**, *36*.
- (4) Lee, K.-W.; Paek, S.; Lien, A.; Durning, C.; Fukuro, H. In *Polymer Surfaces and Interfaces: Characterization, Modification and Application*; Mittal, K. L., Lee K.-W., Eds.; VSP: The Netherlands, 1996; p 1.
- (5) Zhuang, X.; Marrucci, L.; Shen, Y. R. *Phys. Rev. Lett.* **1994**, *73*, 1513.
- (6) Geary, J. M.; Goodby, J. W.; Kmetz, A. R.; Patel, J. S. *J. Appl. Phys.* **1987**, *62*, 4100.
- (7) Seo, D.-S.; Muroi, K.; Isogami, T.; Matsuda, H.; Kobayashi, S. *Jpn. J. Appl. Phys.* **1992**, *31*, 2165.
- (8) van Aerle, N. A. J. M.; Barmantlo, M.; Hollering, R. W. J. *J. Appl. Phys.* **1993**, *74*, 3111.
- (9) Thomas, E. A.; Zupp, T. A.; Fulghum, J. E.; Fredley, D. S.; West, J. L. *Mol. Cryst. Liq. Cryst.* **1994**, *250*, 193.
- (10) Sawa, K.; Sumiyoshi, K.; Hirai, Y.; Tateishi, K.; Kamejima, T. *Jpn. J. Appl. Phys.* **1994**, *33*, 6273.
- (11) Sakamoto, K.; Arafune, R.; Ushioda, S.; Suzuki, Y.; Morokawa, S. *J. Appl. Phys.* **1996**, *80*, 431.
- (12) Ouchi, Y.; Mori, I.; Sei, M.; Ito, E.; Araki, T.; Ishii, H.; Seki, K.; Kondo, K. *Physica B* **1995**, *208/209*, 407.
- (13) Nagayama, K.; Mitsumoto, R.; Araki, T.; Ouchi, Y.; Seki, K. *Physica B* **1995**, *208/209*, 419.
- (14) Mori, I.; Araki, T.; Ishii, H.; Ouchi, Y.; Seki, K.; Kondo, K. *J. Electron. Spectrosc. Relat. Phenom.* **1996**, *78*, 371.
- (15) Samant, M.; Stöhr, J.; Brown, H. R.; Russell, T. P.; Sands, J. M.; Kumar, S. K. *Macromolecules* **1996**, *29*, 8334.
- (16) Toney, M. F.; Russell, T. P.; Logan, J. A.; Kikuchi, H.; Sands, J. M.; Kumar, S. K. *Nature* **1995**, *374*, 709.
- (17) Zhuang, X.; Wilk, D.; Marrucci, L.; Shen, Y. R. *Phys. Rev. Lett.* **1995**, *75*, 2144.
- (18) The sampling depth of 254 eV carbon KVV Auger electrons in polyimide is 1.05 nm. See: Tanuma, S.; Powell C. J.; Penn, D. R. *Surf. Interface Anal.* **1993**, *21*, 165.
- (19) Stöhr, J. *NEXAFS Spectroscopy*; Springer Series in Surface Sciences Vol. 25; Springer: Heidelberg, 1992.
- (20) We are indebted to C. Wöll for a preprint of related work: Weiss, K.; Wöll, C.; Böhm, E.; Fiebranz, B.; Forstmann, G.; Peng B.; Scheumann V.; Johannsmann, D. *Macromolecules* **1998**, *31*, XXX.
- (21) Thulstrup E. W.; Michl, J. *Elementary Polarization Spectroscopy*; VCH Publishers, Inc.: New York, 1989.
- (22) Michinori N.; Yasumasa, T. *Display Imaging* **1995**, *3*, 353.
- (23) Liu, Y.; Russell, T. P.; Samant, M. G.; Stöhr, J.; Brown, H. R.; Cossy-Favre, A.; J. Diaz, J. *Macromolecules* **1997**, *30*, 7768.
- (24) Ishihara, S.; Wakemoto, H.; Nakazima, K.; Matsuo, Y. *Liq. Cryst.* **1989**, *4*, 669.

MA9711708